

Bistability patterns and nonlinear switching with very high contrast ratio in a 1550nm quantum dash semiconductor laser

A. Hurtado, M. Nami, I. D. Henning, M. J. Adams, and L. F. Lester

Citation: *Appl. Phys. Lett.* **101**, 161117 (2012); doi: 10.1063/1.4761473

View online: <http://dx.doi.org/10.1063/1.4761473>

View Table of Contents: <http://apl.aip.org/resource/1/APPLAB/v101/i16>

Published by the [American Institute of Physics](#).

Related Articles

High-power InP quantum dot based semiconductor disk laser exceeding 1.3W

Appl. Phys. Lett. **102**, 092101 (2013)

Chirped InAs/InP quantum-dash laser with enhanced broad spectrum of stimulated emission

Appl. Phys. Lett. **102**, 091102 (2013)

Semiconductor laser monolithically pumped with a light emitting diode operating in the thermoelectrophotonic regime

Appl. Phys. Lett. **102**, 081116 (2013)

Determination of operating parameters for a GaAs-based polariton laser

Appl. Phys. Lett. **102**, 081115 (2013)

GaN-based high contrast grating surface-emitting lasers

Appl. Phys. Lett. **102**, 081111 (2013)

Additional information on *Appl. Phys. Lett.*

Journal Homepage: <http://apl.aip.org/>


Journal Information: http://apl.aip.org/about/about_the_journal

Top downloads: http://apl.aip.org/features/most_downloaded

Information for Authors: <http://apl.aip.org/authors>

ADVERTISEMENT

JANIS Does your research require low temperatures? Contact Janis today.
Our engineers will assist you in choosing the best system for your application.



10 mK to 800 K
Cryocoolers
Dilution Refrigerator Systems
Micro-manipulated Probe Stations

LHe/LN₂ Cryostats
Magnet Systems

sales@janis.com www.janis.com
Click to view our product web page.

Bistability patterns and nonlinear switching with very high contrast ratio in a 1550 nm quantum dash semiconductor laser

A. Hurtado,^{1,2,a)} M. Nami,¹ I. D. Henning,² M. J. Adams,² and L. F. Lester¹

¹Center for High Technology Materials, University of New Mexico, 1313 Goddard St. SE, Albuquerque, New Mexico 87106, USA

²School of Computer Science and Electronic Engineering, University of Essex, Wivenhoe Park, Colchester CO4 3SQ, United Kingdom

(Received 24 July 2012; accepted 5 October 2012; published online 18 October 2012)

We report on the experimental observation of optical bistability (OB) and nonlinear switching (NS) in a nanostructure laser; specifically a 1550 nm quantum dash Fabry-Perot laser subject to external optical injection and operated in reflection. Different shapes of optical bistability and nonlinear switching, anticlockwise and clockwise, with very high on-off contrast ratio (up to 180:1) between output states were experimentally measured. These results added to the potential of nanostructure lasers for enhanced performance offer promise for use in fast all-optical signal processing applications in optical networks. © 2012 American Institute of Physics.

[<http://dx.doi.org/10.1063/1.4761473>]

Bistable semiconductor lasers are expected to form key elements in future optical networks. Thus, the study of optical bistability (OB) and nonlinear switching (NS) in these devices has received considerable attention in the recent past (for a review, see Refs. 1 and 2), and a rich variety of practical applications has been reported. These include all-optical logic gates,^{3–5} all-optical flip-flop,⁶ optical signal regeneration,⁷ optical switching,⁸ wavelength conversion,⁹ optical buffer memory,¹⁰ etc. The range of laser structures where OB and NS has been investigated includes devices with bulk or quantum-well (QW) active regions, such as edge-emitting lasers, Fabry-Perot (FP)^{11–13} and distributed feedback (DFB)^{8,14,15} and also vertical-cavity devices, i.e., vertical cavity surface emitting lasers (VCSELs),^{16,17} and vertical cavity semiconductor optical amplifiers (VCSOAs)^{18–20} (for a review see Refs. 1 and 2 and references therein).

In addition, the analysis of optically injected nanostructure lasers, including quantum dot (QDot) and quantum dash (QDash) lasers has undergone important research effort in recent years and several works have analysed the injection locking and nonlinear dynamics occurring in such devices.^{21–24} However, the study of OB and NS in nanostructure lasers has not yet attracted much attention despite their theoretically superior properties. Devices made using advanced QDot or QDash active regions offer many potential advantages including ultrafast carrier dynamics,²⁵ reduced linewidth enhancement factor (α),²⁶ and low temperature dependence of the threshold current.²⁷ The practical performance gains which accrue from the realisation of these advantages ensure that nanostructure semiconductor lasers will play a key role as high-performance sources in a variety of future applications. One such aspect forms the focus of the present work, which investigates the bistability and switching properties in nanostructure lasers. In particular, we report the experimental observation of different shapes of OB and NS, anticlockwise and clockwise, with very high on-off contrast ratio (up to 180:1) in a QDash FP laser. The

reported results observed in a nanostructure laser at the important telecom wavelength of 1550 nm offer prospects for the use of these devices in all-optical signal processing applications in optical networks.

Fig. 1(a) shows the experimental setup used in this work. Light from a 1550 nm tuneable laser (master laser, ML) was injected into a 500- μm long QDash FP laser (slave laser, SL) operated in reflection. An erbium doped fibre amplifier (EDFA) amplifies the signal coming from the ML. With this configuration, an external optical signal with power levels up to 25 mW was injected into the SL. A narrow band-pass optical filter was used to remove the EDFA's added amplified spontaneous emission noise. A variable optical attenuator (VOA) is used to control the optical power of the external signal. Light is injected into the SL via a three-port polarisation maintaining (PM) optical circulator and a 99/1 PM optical coupler. The 1% port of the coupler is connected to a power meter for the monitoring of the optically injected power, whereas the 99% port is directly connected to the SL. The light reflected by the SL is collected from the third port of the PM circulator and analysed with an optical spectrum analyser (OSA). A lens-ended fibre with estimated coupling losses of 6 dB was used to couple light in and out the QDash laser.

The epitaxial layer structure of the QDash laser used in this work is shown in Fig. 1(b). The active region consists of 5 layers of InAs quantum dashes embedded in strained $\text{Al}_{0.20}\text{Ga}_{0.16}\text{In}_{0.64}\text{As}$ quantum wells separated by 30 nm of undoped tensile-strained $\text{Al}_{0.28}\text{Ga}_{0.22}\text{In}_{0.50}\text{As}$ spacers. This configuration is usually referred to as dashes-in-a-well or DWELL. The length and width of the laser cavity are respectively 500 μm and 4 μm with cleaved facets providing an approximated reflectivity of 30%. Fig. 1(c) plots the measured LI (Light vs. Current) curve of the device at 293 K showing a threshold current (I_{th}) of 53 mA. An optical power of 0.925 mW was measured for the device biased with 80 mA, which accounting for the coupling losses introduced by the lensed fibre gives an estimated total emitted power of 3.7 mW at that current. The spectrum (biased with 70 mA at

^{a)}E-mail addresses: ahurta01@unm.edu and ahurt@essex.ac.uk.

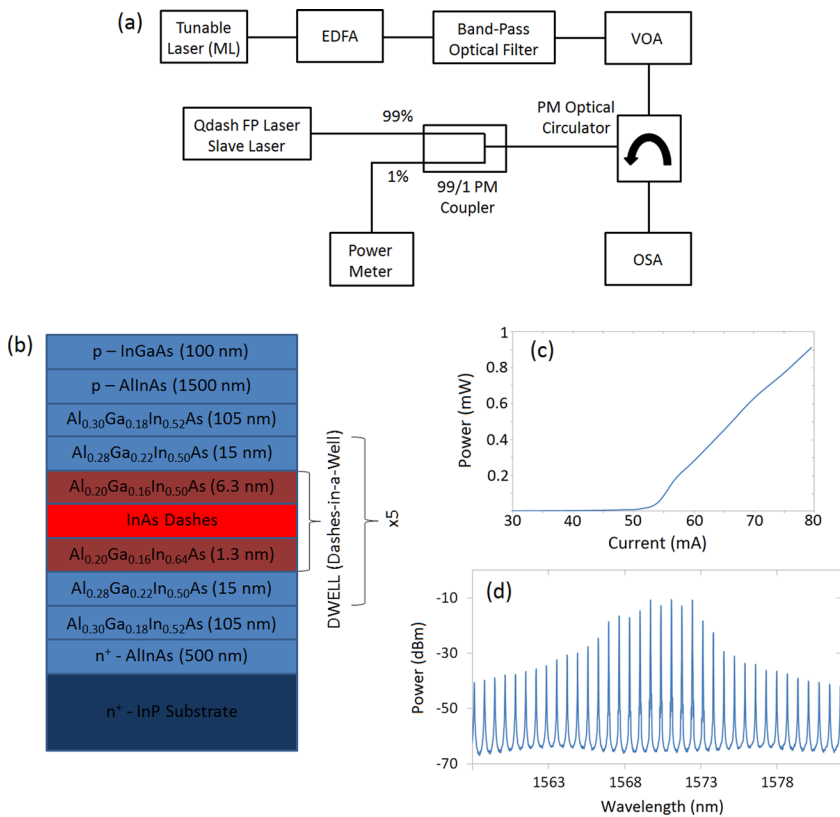


FIG. 1. (a) Experimental setup used in this work. (b) Epitaxial layer composition of the 1550 nm-QDash FP laser. (c) Optical spectrum at 70 mA and (d) LI (Light vs. current) curve of the device; both plots at 293 K. EDFA = erbium doped fibre amplifier; VOA = variable optical attenuator; and OSA = optical spectrum analyzer.

293 K) is included in Fig. 1(c) showing the different longitudinal modes separated by approximately 0.7 nm and with main emission wavelength around 1570 nm. Other parameter values measured for analogous devices to that used in this work include an slope efficiency of 0.1 W/A (see the inset in Fig. 1 in Ref. 28), internal loss of 14 cm⁻¹ (Fig. 2(b) in Ref. 29), and a linewidth enhancement factor (α) of 1.7 at a current of 60mA (as seen in Fig. 5 in Ref. 30 plotting the evolu-

tion of α with bias current). For complete details on the device structure, see for instance Refs. 28–30.

Figs. 2(a)–2(e) show the reflected/injected optical power relationships of the 1550 nm-QDash FP laser when the device is biased with a current of 60 mA ($1.13 \times I_{th}$). Results are plotted for different values of initial wavelength detuning between ML and SL ($\Delta\lambda = \lambda_{ML} - \lambda_{SL}$) from 0.052 nm to 0.355 nm. Blue diamonds and red squares in Figs. 2(a)–2(e)

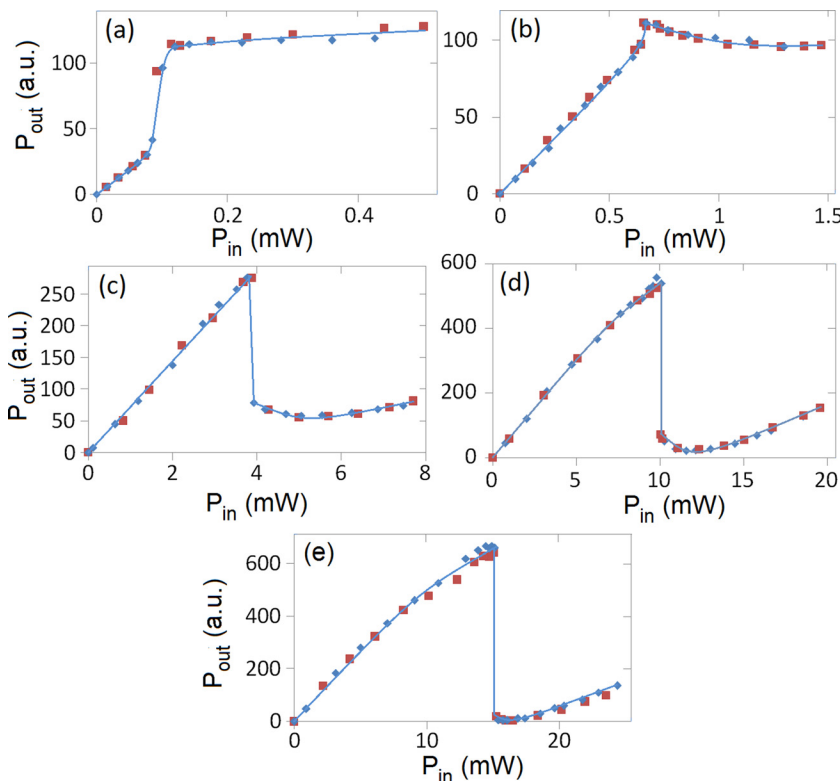


FIG. 2. Reflected vs. input power; the QDash laser is biased with 60mA. Four different values of detuning are configured between ML and SL: (a) 0.052, (b) 0.1, (c) 0.205, (d) 0.3, and (e) 0.355 nm.

correspond, respectively, to measured results for increasing and decreasing values of injected power. The results in Figs. 2(a)–2(e) show in all cases the attainment of an abrupt switching transition between two different stable states. This switching occurs after a particular threshold in injected power is exceeded. This threshold value coincides with the situation where the SL locks to the ML. Figs. 2(a)–2(e) also show that progressively higher initial detuning results in higher input power requirements for the attainment of the switching transition. Such behaviour is due to the need to pull the SL's resonant wavelength further to lock to the ML's wavelength. Figs. 2(a)–2(e) also reveal the appearance of different patterns for the nonlinear switching transition. For low enough values of initial detuning, Fig. 2(a) shows a situation where a switching transition from a lower to higher amplitude output state is produced. Such behaviour is usually referred as anticlockwise nonlinear switching.^{1,11,19,20} As the configured detuning is increased, the contrast ratio between switching states reduces. Still, anticlockwise nonlinear switching is observed when the detuning between ML and SL is equal to 0.1 nm, as shown in Fig. 2(b). Greater values of $\Delta\lambda$ are translated into a further reduction of contrast ratio until the switching transition changes direction.^{11,12,19,20} Now, the output of the QDash FP laser transits abruptly from a higher to a lower amplitude state; thus clockwise nonlinear switching is attained at the reflective output of the device.

Such response can be observed in Figs. 2(c)–2(e) when higher values of initial wavelength detuning from 0.205 to 0.355 are configured.

Figs. 3(a)–3(e) show the reflected/injected optical power relationships of the 1550 nm-QDash FP laser with the device biased with a higher current of 80 mA ($\approx 1.5 \times I_{th}$). Measurements are plotted for different initial wavelength detunings between the ML and SL, as indicated in the caption of Fig. 3. Again, blue diamonds and red squares in Figs. 3(a)–3(e) correspond, respectively, to measured results for increasing and decreasing injected optical power. Important similarities can be observed between the results in Figs. 3(a)–3(e) and those depicted in Figs. 2(a)–2(e). For a higher biasing case, Figs. 3(a)–3(e) also show the occurrence of different switching transitions as the initial detuning was increased from 0.052 to 0.355 nm. Anticlockwise nonlinear switching occurs for low values of detuning, as seen in Figs. 3(a) and 3(b). Figs. 3(c)–3(e) show in turn a change of the switching transition from anticlockwise to clockwise when the initial detuning is further increased. However, the results in Figs. 3(c)–3(f) exhibit an important difference from those obtained for a lower applied bias current closer to the value at threshold (see Figs. 2(c)–2(e)). Now, a hysteresis cycle appears associated with the switching transition, and, therefore, OB is attained in the reflective output of the device. Since the hysteresis cycle appears accompanying a switching transition in the clockwise

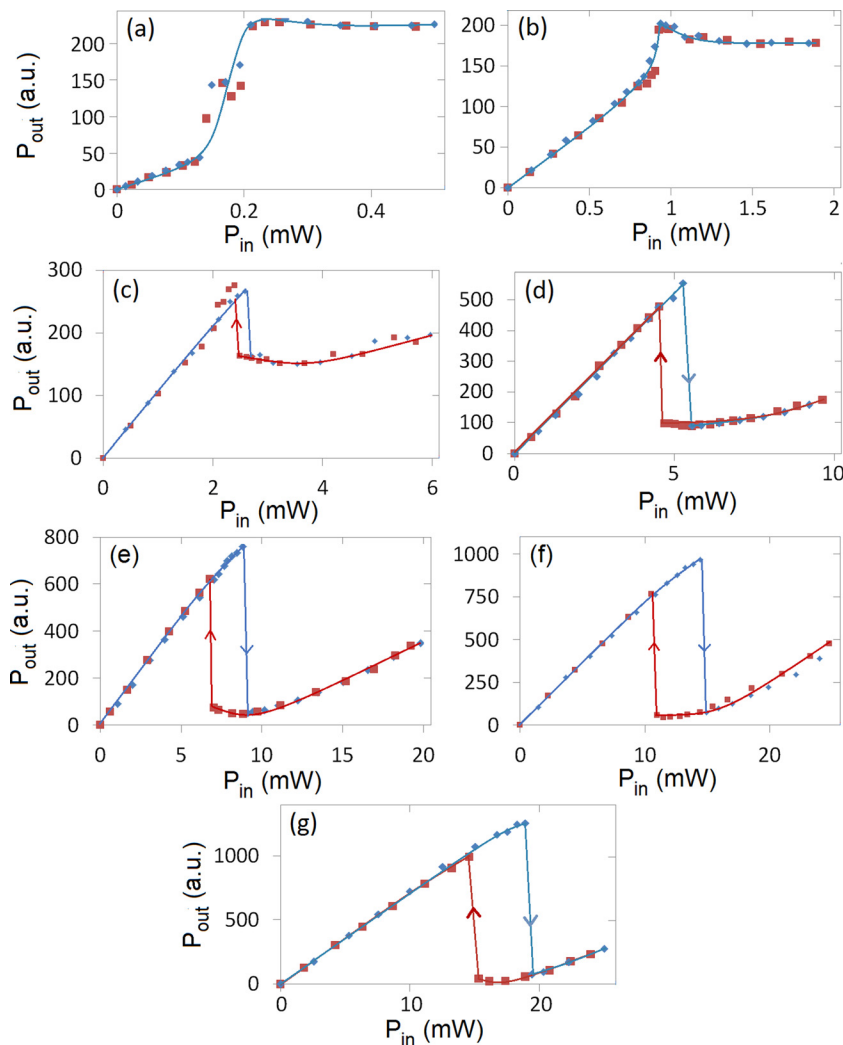


FIG. 3. Reflected vs. Input power; the QDash laser is biased with 80mA. Four different values of detunings are configured between ML and SL: (a) 0.055, (b) 0.102, (c) 0.15, (d) 0.2, (e) 0.25, (f) 0.3, and (g) 0.35 nm.

direction, this behaviour is usually referred as clockwise optical bistability.^{11,12,19,20}

These behaviours are also illustrated in Figs. 4(a) and 4(b), which plots the optical power levels needed to produce the switching-up and switching-down transitions as a function of the initial wavelength detuning for the two biasing cases (60 and 80 mA). Fig. 4(a) shows that for all values of detuning, the switching-up and switching-down points are equal, independent of increasing or decreasing the externally injected optical power. No hysteresis associated with the switching is produced and only NS (anticlockwise or clockwise) is measured. In contrast, Fig. 4(b) shows a different behaviour. Now, for low values of detuning, equal switching-up and switching-down points are measured when anticlockwise nonlinear switching is produced (as seen in Figs. 3(a) and 3(b)). However, as the detuning is further increased the switching-up and switching-down points start differing. This indicates the existence of a hysteresis cycle associated with the switching transition and, therefore, the attainment of bistability. The width of the hysteresis cycle is determined by the area encompassed by the measured switching-up and -down points, and as seen in Fig. 4(b), OB with a wider hysteresis cycle is obtained as the initial detuning is increased.

In turn, Figs. 4(c) and 4(d) show, respectively, for both biasing cases (60 and 80 mA), the measured on-off contrast ratio between switching states as a function of the initial wavelength detuning. In both cases, for low values of detuning, when anticlockwise nonlinear switching occurs, relatively low values of on-off contrast ratio around 5:1 are measured. The on-off contrast ratio then reduces until the switching transition changes shape from anticlockwise to clockwise. After that inflection point, a rapid growth of the on-off contrast ratio is measured with increased detuning, as Figs. 4(c) and 4(d) show. This situation corresponds to the occurrence of clockwise nonlinear switching when the applied bias current was closer to threshold (60 mA) or clockwise bistability for a higher current (80 mA) well above the threshold of the device. Encouragingly, very high values for the on-off contrast ratio for this clockwise NS and OB, as high as 180:1 at 60 mA (Fig. 4(c)) and in excess of 50:1 for 80 mA (Fig. 4(d)) were measured. These record values of reflective optical power switching and bistability are at least

one order of magnitude higher than any previously reported for other types of semiconductor lasers and laser amplifiers including bulk or quantum well edge-emitting or vertical-cavity devices.^{11–19} We must note that the peak power of the reflective signal was used to determine the on-off contrast ratio. We believe that this technique is in fact conservative. Before switching, the QDash laser emits in many longitudinal modes and the total power (all modes) is thus higher than the measured peak power (one mode). After switching, only the injected mode is present, since the low amplitude state in reflection corresponds to the locked, high intensity state in the cavity, and the total and peak power would be of comparable magnitudes. Hence, the on-off contrast ratio would be even higher if the total reflected power was measured.

The results obtained in this work with a 1550 nm-QDash FP laser demonstrate significant differences with those previously reported in other types of edge-emitting devices, including bulk or QW active region devices.^{11–15} The latter showed anticlockwise OB with very wide hysteresis cycles, even for low values of initial detuning and for applied bias currents very close to threshold or below that level.^{11–13} Furthermore, for edge-emitting devices biased above threshold, anticlockwise OB had only been reported,¹³ while the occurrence of clockwise or other types of bistability has only been measured when biased below threshold.^{11,12} Surprisingly, the results obtained with a nanostructure QDash FP laser show stronger similarities to those reported for QW vertical-cavity devices, VCSELs and VCISOAs,^{16–19} with completely different structure and characteristics compared to the QDash FP laser used in this work. In those works with QW vertical-cavity devices, clockwise NS and OB were also observed as the initial detuning was increased.^{17–20}

We believe there are two important factors explaining these emerging differences with previous results in edge-emitting lasers as well as the similarities with results reported for vertical-cavity devices. First, the relatively lower values of linewidth enhancement factor (α) reported for nanostructure lasers³⁰ comparable to those reported for QW VCSELs.³¹ Specifically, for an analogous device to that used in this work, a value of α of only 1.7 was measured at 60 mA; with increasing value of α as the applied bias current grows. Higher values of α result in the easier occurrence of

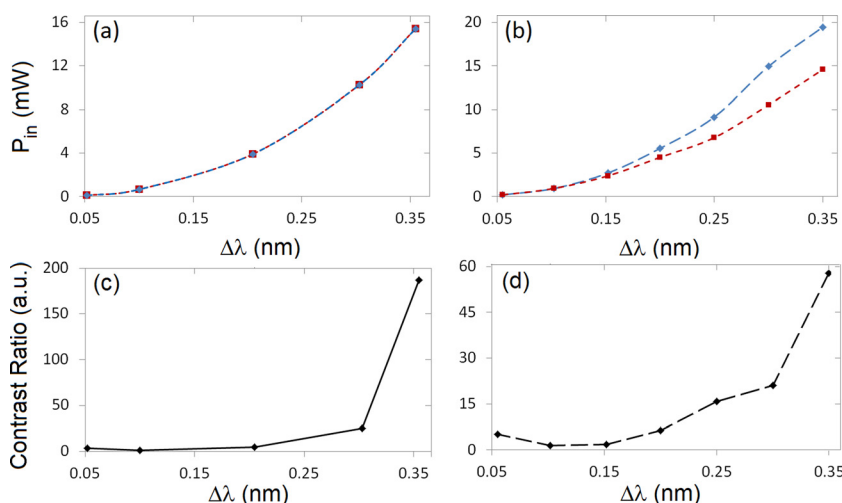


FIG. 4. (a) and (b) Switching-up/down points and (c) and (d) contrast ratio vs. $\Delta\lambda$. The SL is biased with (a) and (c) 60 and (b) and (d) 80 mA.

bistability with wider hysteresis cycles.^{1,11,17} With the QDash laser of this work, higher levels of initial wavelength detuning and bias current are needed to achieve bistability, otherwise nonlinear switching occurs. This is exactly the same behaviour observed in QW VCSELs and VCISOAs, devices also exhibiting low values of α .^{16,20}

We also believe that the reduced areal coverage of the active region of nanostructure lasers plays an important role in the observed results. In bulk and QW planar lasers, the active region occupies the whole cavity length. However, in a QDash nanostructure laser, the active region occupies a relatively small portion of the cavity resulting in lower maximum gain. For the particular laser discussed here, this means that the device must be pumped to high current density (2.65 kA/cm² at threshold) and a correspondingly strong population inversion. This is the same scenario in QW VCSELs and VCISOAs with the active region occupying just a small portion of the total internal cavity volume. In such devices, due to the small dimensions of the active region, an externally injected optical signal experiences reduced gain as it propagates along the cavity; this ultimately determines the shape of the switching transition causing it to turn to the clockwise direction.^{11,19,20} Hence, we believe that the QDash nanostructure laser of this work presents a similar physical condition for the attainment of clockwise nonlinear switching and bistability as in vertical-cavity devices.^{17–20}

In conclusion, in this work, we report the experimental observation of OB and NS in a nanostructure laser; specifically, a 1550-nm-QDash FP semiconductor laser subject to external optical injection and operated in reflection. Different patterns of switching and bistability, anticlockwise and clockwise, were experimentally measured. Furthermore, very high values of on-off contrast ratio between switching states (up to 180:1) were also measured. These encouraging results obtained with a QDash nanostructure laser operating at the important telecom wavelength of 1550 nm, besides the potential for fast operating speed and enhanced performance, offer promise for their use in all-optical signal processing applications in telecommunication networks.

This work has been funded in part by the European Commission under the Programme FP7 Marie Curie International Outgoing Fellowships (IOF) Grant PEOF-GA-2010-273822 and the Air Force Research Grants FA9550-10-1-0276 and FA9550-12-1-0049.

¹M. J. Adams, A. Hurtado, D. Labukhin, and I. D. Henning, *Chaos* **20**, 037102 (2010).

²H. Kawaguchi, *Bistabilities and Nonlinearities in Laser Diodes* (Artech House, Norwood, MA, 1994).

- ³A. Quirce, J. R. Cuesta, A. Hurtado, K. Schires, A. Valle, L. Pesquera, I. D. Henning, and M. J. Adams, *IEEE J. Quantum Electron.* **48**, 588 (2012).
- ⁴A. Hurtado, A. P. Gonzalez-Marcos, and J. A. Martin-Pereda, *Proc. SPIE* **5577**, 58 (2004).
- ⁵P. Wen, M. Sanchez, M. Gross, and S. Esener, *Opt. Commun.* **219**, 383 (2003).
- ⁶K. Huybrechts, T. Tanemura, Y. Nakano, R. Baets, and G. Morthier, *IEEE Photon. Technol. Lett.* **21**, 703 (2009).
- ⁷K. Inoue and M. Yoshino, *IEEE Photon. Technol. Lett.* **7**, 164 (1995).
- ⁸A. Hurtado, I. D. Henning, and M. J. Adams, *IEEE Proc.-J: Optoelectron.* **153**, 21 (2006).
- ⁹D. N. Maywar, Y. Nakano, and G. P. Agrawal, *IEEE Photon. Technol. Lett.* **12**, 858 (2000).
- ¹⁰J. Sakaguchi, T. Katayama, and H. Kawaguchi, *Opt. Express* **18**, 12362 (2010).
- ¹¹P. Pakdeevanich and M. J. Adams, *IEEE J. Quantum Electron.* **35**, 1894 (1999).
- ¹²N. F. Mitchell, J. O’Gorman, J. Hegarty, and J. C. Connolly, *Opt. Lett.* **19**, 269 (1994).
- ¹³P. Pakdeevanich and M. J. Adams, *Opt. Commun.* **176**, 195 (2000).
- ¹⁴M. J. Adams and R. Wyatt, *IEEE Proc.-J: Optoelectron.* **134**, 35 (1987).
- ¹⁵D. N. Maywar and G. P. Agrawal, *IEEE J. Quantum Electron.* **33**, 2029 (1997).
- ¹⁶K. H. Jeong, K. H. Kim, S. H. Lee, M. H. Lee, B. S. Yoo, and K. A. Shore, *IEEE Photon. Technol. Lett.* **20**, 779 (2008).
- ¹⁷A. Hurtado, I. D. Henning, and M. J. Adams, *IEEE J. Sel. Top. Quantum Electron.* **14**, 911 (2008).
- ¹⁸C. R. Marki, D. R. Jorgesen, H. J. Zhang, P. Y. Wen, and S. C. Esener, *Opt. Express* **15**, 4953 (2007).
- ¹⁹A. Hurtado, I. D. Henning, and M. J. Adams, *Appl. Phys. Lett.* **91**, 151106 (2007).
- ²⁰A. Hurtado, A. Gonzalez-Marcos, and J. A. Martin-Pereda, *IEEE J. Quantum Electron.* **41**, 376 (2005).
- ²¹J. F. Hayau, O. Vaudel, P. Besnard, F. Lelarge, B. Rousseau, L. Le Gouezigou, F. Pommereau, F. Poingt, O. Le Gouezigou, A. Shen, D. Guang-Hua, O. Dehaese, F. Grillot, R. Piron, S. Loualiche, A. Martinez, K. Merghem, and A. Ramdane, CLEO Europe—EQEC 2009 Conference, Munich, Germany, 2009.
- ²²T. Erneux, E. A. Viktorov, B. Kelleher, D. Goulding, S. P. Hegarty, and G. Huyet, *Opt. Lett.* **35**, 937 (2010).
- ²³E. Sououdi, G. Huyet, J. G. McInerney, F. Lelarge, K. Merghem, R. Rosales, A. Martinez, A. Ramdane, and S. P. Hegarty, *IEEE Photon. Technol. Lett.* **23**, 1544 (2011).
- ²⁴B. Kelleher, D. Goulding, S. P. Hegarty, G. Huyet, E. A. Viktorov, and T. Erneux, *Optically Injected Single-Mode Quantum Dot Lasers in Quantum Dot Devices* (Springer, NY, 2012), Chap. 1, pp. 1–22.
- ²⁵P. Bhattacharya, D. Klotzkin, O. Qasaimeh, W. Zhou, S. Krishna, and D. Zhu, *IEEE J. Sel. Top. Quantum Electron.* **6**, 426 (2000).
- ²⁶H. Y. Liu, T. J. Badcock, K. M. Groom, M. Hopkinson, M. Gutiérrez, D. T. Childs, C. Jin, R. A. Hogg, I. R. Sellers, D. J. Mowbray, M. S. Skolnick, R. Beanland, and D. J. Robbins, *Proc. SPIE* **6184**, 618417 (2006).
- ²⁷T. C. Newell, D. J. Bossert, A. Stintz, B. Fuchs, K. J. Malloy, and L. F. Lester, *IEEE Photon. Technol. Lett.* **11**, 1527 (1999).
- ²⁸F. Grillot, N. A. Naderi, M. Pochet, C.-Y. Lin, and L. F. Lester, *Appl. Phys. Lett.* **93**, 191108 (2008).
- ²⁹C.-Y. Lin, Y.-C. Xin, Y. Li, F. L. Chiragh, and L. F. Lester, *Opt. Exp.* **17**, 19739 (2009).
- ³⁰N. A. Naderi, M. Pochet, F. Grillot, N. Terry, V. Kovanis, and L. F. Lester, *IEEE J. Sel. Top. Quantum Electron.* **15**, 563 (2009).
- ³¹N. A. Khan, K. Schires, A. Hurtado, I. D. Henning, and M. J. Adams, *IEEE J. Quantum Electron.* **48**, 712 (2012).